



## ROOM TEMPERATURE SYNTHESIS OF CERIA BY THE ASSISTED OF CATIONIC SURFACTANT AND AGING TIME

(Sintesis Ceria Pada Suhu Bilik Dengan Bantuan Surfaktan Kation Dan Masa Penuaan)

Nor Aqilah Mohd Fadzil<sup>1\*</sup>, Mohd Hasbi Ab. Rahim<sup>1</sup>, Gaanty Pragas Maniam<sup>2</sup>

<sup>1</sup>Faculty of Industrial Science & Technology

<sup>2</sup>Central Laboratory

Universiti Malaysia Pahang, Lebuhraya Tun Razak, 26300 Gambang, Kuantan, Pahang, Malaysia

\*Corresponding author: [Aqilah\\_mawaddah@yahoo.com](mailto:Aqilah_mawaddah@yahoo.com)

Received: 14 January 2018; Accepted: 8 May 2018

### Abstract

This paper presents the synthesis of rare earth cerium(IV) oxide (ceria) via simple precipitation method under room temperature. The two aims of this research are to: (i) synthesise a ceria-based material using simple process and chemicals and (ii) modify the ceria-based material with environmentally friendly elements. In this study, cerium nitrate hexahydrate and sodium hydroxide were utilised as the precursor and precipitant, respectively, to attain desired crystallite size and shape, at a fixed reaction pH of 12. Besides that, common cationic surfactant, cetyl-tri-methyl-ammonium bromide (CTAB), was used to enhance ceria-based material's coveted properties. Furthermore, addition of surfactant and aging time (30 minutes, and 5, 10, 20, and 30 days) were also examined. Findings showed that as aging time increased, crystallite size decreased and production of large agglomerations were not observed. Then, optimum aging time was applied for synthesis of ceria material and modified ceria material, Fe-CeO<sub>2</sub>/TiO<sub>2</sub>, via impregnation method. These materials were subjected to X-ray diffraction (XRD), CO<sub>2</sub>-Temperature-Programmed Desorption (CO<sub>2</sub>-TPD), and Field Emission Scanning Electron Microscopy (FESEM) to investigate the mutual effect of surfactant addition and aging time.

**Keywords:** cationic, ceria, crystallite, precipitating, surfactant

### Abstrak

Kajian ini menggambarkan sintesis salah satu unsur nadir bumi iaitu cerium(IV) oksida (ceria), melalui kaedah pemendakan pada suhu bilik. Matlamat kajian ini ialah: (i) sintesis bahan berasaskan ceria menggunakan proses dan bahan kimia yang mudah dan (ii) mengubahsuai bahan berasaskan ceria dengan penambahan unsur-unsur mesra alam. Dalam kajian ini, cerium nitrat heksahidrat dan natrium hidroksida telah digunakan sebagai bahan pemula dan agen pemendakan, supaya saiz dan bentuk yang dikehendaki dapat diperolehi pada pH yang telah ditetapkan iaitu pH 12. Selain itu, bahan tipikal surfaktan kation, cetil-tri-metil-ammonium bromida (CTAB), telah digunakan untuk memudahkan penghasilan bahan berasaskan ceria dengan sifat-sifat yang dikehendaki. Di samping itu, penambahan surfaktan dan kadar masa penuaan (30 minit, dan 5, 10, 20, dan 30 hari) turut dikaji. Hasil penemuan menunjukkan bahawa, apabila kadar masa penuaan ditingkatkan, saiz kristal berkurangan dan penghasilan gumpalan besar tidak ditemui. Justeru, kadar masa penuaan optima dipilih untuk sintesis bahan ceria dan bahan ceria yang diubah suai, Fe-CeO<sub>2</sub>/TiO<sub>2</sub>, melalui kaedah impregnasi. Seterusnya, bahan-bahan ini dianalisis melalui sistem pembelauan sinar-X (XRD), program penjerap bersuhu-CO<sub>2</sub> (CO<sub>2</sub>-TPD), dan mikroskop elektron pengimbas pancaran medan (FESEM) untuk mengkaji kesan penambahan surfaktan dan kadar masa penuaan.

**Kata kunci:** kation, ceria, kristal, pemendakan, surfaktan

### Introduction

Rare earth elements are an interesting prospect for research due to its potential of application in many areas, including catalysis, UV absorbance, medical/bio-sensing, and gas and solar sensors [1, 2]. Cerium is one such element, possessing great prospects in the chemical-based industry. Its electronic configuration's versatility (Xe 4f<sup>1</sup> 5d<sup>1</sup> 6s<sup>2</sup>) is a unique feature that allows electrons to move freely from similar energy level orbitals between 4f<sup>1</sup> and 5d<sup>1</sup>. This results in positive contributions, especially in catalytic reactions.

Moreover, upon combination with oxygen, cerium oxide (CeO<sub>2</sub>; ceria) is formed, with a composition ratio of 1:2 (cerium; oxygen). This attributes for its oxygen storage capacity (OSC). Ceria can oxidise and/or reduce any material that comes into contact with its surface. Oxygen vacancy defects will immediately form, which is a necessity, especially during catalytic processes. A faster and increased formation of oxygen vacancy defects results in high OSC, making ceria a superior material for oxidation/reduction processes [3].

Ceria can be synthesised via various techniques, including ones involving surfactant media. By applying surfactant during synthesis, good properties pertaining to ceria's crystallite size and morphology can be facilitated, resulting in better performance in certain applications. Ceria prepared in a surfactant media forms a clear shape (e.g. sphere, nanorods) and possesses a significantly larger surface area (>130 m<sup>2</sup>/g) compared to an analogue sample devoid of surfactant [4]. Thus, in the absence of surfactant during synthesis, an irregularly shaped ceria with a small surface area (≈50 m<sup>2</sup>/g) was formed. Additionally, ceria preparation in a surfactant media is typically combined with specific aging time (<30 days). Generally, nanoparticle formation occurs in a short time, but application of aging time extends its growth. The particles will stack among themselves to grow directionally [5].

The formation of 1-D nanostructured ceria could be easily performed in the presence of a surfactant. This situation is termed soft template assisted. Apart from cetyl-tri-methyl-ammonium bromide (CTAB), other surfactants that can be used as a soft template are alkyltrimethylammonium salts, octadecylamine, and ethylenediamine. In the primary stage, addition of cerium precursor salts into a basic condition will form hydrous cerium oxide. Then, due to presence of the template, hydrous cerium oxide will react with organic molecules through exchange of OH<sup>-</sup> group on the surface. Next, hydrous cerium oxide may undergo an exchange with either a cation or anion. Nevertheless, this process is pH dependent. Hence, if the pH is higher than the isoelectric point of hydrous cerium oxide (pH: 6.75 to 8.00), exchange of OH<sup>-</sup> group with the surfactant's cation will take place [6, 7]. The higher surface area of Ce(IV) will result in a smaller nanoparticle size. Furthermore, presence of surfactant will also assist in oxidation of cerium(III) to cerium(IV) [8].

Surfactant addition can also manipulate the shape of 1-D ceria produced. Specifically, by controlling ratio of surfactant to cerium precursor, from 1.0:1.0 to 1.5:1.0, shape of ceria nanoparticles might change from spherical to nanorod. Nonetheless, this effort must be accompanied by well-controlled temperature, pH, and effective reaction time [9]. At a lower temperature, i.e. <150 °C, nanorod morphology cannot be formed. This is because temperature of <150 °C could not assist in nucleation growth of particles. Moreover, previous studies [10–12] that demonstrated the single step of producing ceria nanorod structure, revealed that it involves a complicated and non-environmentally friendly approach. This is due to high temperature (>150 °C) and long reaction time needed to yield ceria's nanorod structure.

In general, the morphology of 1-D nanostructured ceria could be briefly explained as follows. First, under a basic condition, cerium will be oxidised into hydrated Ce<sup>4+</sup>. Then, this hydrated molecule readily reacts with CTAB surfactant, producing polymeric hydrous oxide. If the reaction pH is above the isoelectric point of ceria, i.e. above pH 8, polymeric hydrous oxide will react with alkylammonium salt. During this reaction, surfactant and deprotonated hydroxyl group will generate an inorganic/organic composite [13]. This composite is the primary cause for cerium oxide's high surface area (>100 m<sup>2</sup>/g). Typically, products with a high surface area are formed due to efficient drying or calcination process. Therefore, during drying or calcination process, surfactant will play a key role in formation of nanostructured ceria. For example, a lower surfactant amount will usually result in a shorter length for ceria nanostructure [14].

The main role of a surfactant is to facilitate a favourable site for growth of particulate assemblies between cerium cation and surfactant micelle. This influences the morphology and formation processes like nucleation, growth, and coagulation. However, presence of surfactant alone is futile. Instead, it should be accompanied by aging time factor. Aging time varies from an hour up to a couple of weeks. Yang and Guo [15] suggested that a short aging time (30 minutes to 7 days) will induce the colloidal solution to predominantly contain  $\text{Ce}^{4+}$ . Meanwhile, for a long aging time (8 to 30 days), the colloidal solution will contain ceria nanoparticles and  $\text{Ce}^{4+}$ . Nevertheless, this situation may change based on different surfactant and reaction conditions applied.

As previously mentioned, with a long aging time, the oxidation state of cerium will change along with its particle size. Changes in oxidation state will modify adsorption capability and band gap measurement, resulting in different electrochemistry properties of ceria [16]. Nonetheless, an overlong aging time is undesirable, since the particles will start to disappear due to unstable condition. Besides that, if the colloidal solution is left too long for aging time purpose, the pH of the solution will turn acidic because of slow adsorption of  $\text{CO}_2$  gas into it.

On the other hand, generation of ceria nanorod structure could still be achieved without addition of surfactants. Lin and Chowdhury [17] demonstrated the application of a well-known hydrothermal synthesis technique at a higher concentration of sodium hydroxide ( $\text{pH} > 10$ ). This method was conducted for 24 hours and successfully produced 1-D nanorod structure with 20–40 nm and 200–300 nm of diameter and length, respectively. Furthermore, this ceria nanorod structure was obtained through drying overnight in an oven at 60 °C followed by calcination at 300 °C for 3 hours, in the presence of air.

As such, this study incorporates both surfactant application and aging time for modification of ceria into Fe- $\text{CeO}_2/\text{TiO}_2$  nanoparticle. Ceria is typically used for active support, as numerous research findings have indicated that such a characteristic is due to strong metal-ceria surface defects bonding, which stabilises the metal catalyst [18–22]. In this situation, ceria-metal interface will exist through oxygen migration from the support to the metal and vice versa, resulting in an enhanced surface reaction (e.g. catalysis). Thus, applying ceria as the main element in Fe- $\text{CeO}_2/\text{TiO}_2$  nanoparticle is expected to boost oxygen migration and display excellent catalytic performance. However, this work will only focus on characteristics of the developed Fe- $\text{CeO}_2/\text{TiO}_2$  nanoparticles.

### **Materials and Methods**

Cerium nitrate hexahydrate (Sigma-Aldrich, Missouri, USA) and sodium hydroxide (Sigma-Aldrich, Missouri, USA) were utilised as the precursor and precipitant agent, respectively. In settings requiring surfactant media, cationic surfactant CTAB (Sigma-Aldrich, Missouri, USA) was utilised, whereas metal loading and catalyst support were provided by iron nitrate hexahydrate (Sigma-Aldrich, Missouri, USA) and titanium dioxide (Sigma-Aldrich, Missouri, USA), respectively.

#### **Synthesis of ceria nanoparticles via simple precipitation method**

Simple precipitation technique was used to produce ceria nanoparticles. The concentration ratio of 3:1 (CTAB: cerium precursor) was prepared in 100 mL deionised water (DI), at pH 12 and at room temperature. Firstly, 6.5 g of CTAB was dissolved in 100 mL DI water, and then 2.6 g of cerium precursor was added with vigorous stirring. After the solution became homogeneous, precipitant sodium hydroxide solution (0.5 M) was added drop by drop until pH 12 was achieved. Subsequently, the solution was kept under vigorous stirring for 2 hours and left for aging (at  $t = 30$  minutes and 3, 5, 10, 20, and 30 days). Finally, the solution was filtered and washed thrice using DI water, followed by drying in the oven for 3 hours at 70 °C.

#### **Synthesis of Fe- $\text{CeO}_2/\text{TiO}_2$ nanoparticle via impregnation method**

The modified ceria material, Fe- $\text{CeO}_2/\text{TiO}_2$ , was synthesised using impregnation method, in which different total metal loadings of 0.5, 1.0, 3.0, and 5.0 wt.% were applied. First, 0.25 g of  $\text{FeCl}_2 \cdot 4\text{H}_2\text{O}$  was added to 30 mL DI water, with the solution being kept under vigorous stirring and mild heating (40 °C). Then, 1.9 g  $\text{TiO}_2$  and ceria mixture were physically mixed and grinded before being added into the iron solution under vigorous stirring. Next, the reaction mixture was covered using an aluminium foil with many small holes and dried overnight in an oven at 100 °C. Before sending the sample for characterisation, it was first calcined using a horizontal furnace for 3 hours at 400 °C, with a heating rate of 40 °C/min.

### Characterisation

The sample powder's crystallite size was obtained using Rigaku Miniflex X-ray Diffractometer (XRD). The X-ray of the Cu K $\alpha$  radiation was filtered by a Ni filter with  $\lambda=1.54$  Å, whereas Scherrer's formula (equation (1)) was utilised to determine crystallite size [22]. In Scherrer's formula, C indicates a numerical constant ( $\approx 0.9$ ). The wavelength of X-ray was 1.5418 Å for Cu K $\alpha$  radiation. Meanwhile,  $\beta$  and  $\theta$  were the full width at half maximum (FWHM) in radians and diffraction angle for the peak, respectively.

$$\text{Crystallite size} = C\lambda / \beta \cos\theta \quad (1)$$

Morphological studies for the prepared sample were done using Field Emission Scanning Electron Microscope (FESEM), model JSM-8700F. The sample was coated with platinum and/or gold. Besides that, elemental analysis was conducted using Energy Dispersive X-ray Analysis (EDX) FEI Quanta 450, while CO<sub>2</sub>-Temperature Programmed Desorption (CO<sub>2</sub>-TPD) was carried out to examine the sample's surface basicity. TPDRO 1100 Series Thermo Finnigan was purged with helium gas before commencing analysis.

## Results and Discussion

### Percentage yield

Reaction time under vigorous stirring was set for 2 hours, however, no significant advantage in percentage yield was observed when time was extended to 4, 8, 24, and 48 hours. As shown in Table 1, reaction time did not greatly influence percentage yield of ceria nanoparticles, indicating that 2 hours is the optimum reaction time for the process. Results also indicated that stirring rate was proportional to percentage yield. A slow stirring rate showed a low percentage yield, while as it increased up to 1200 rpm, percentage yield increased twofold. Moreover, at the high stirring rate, the solution turned yellowish in colour. High stirring rate could have induced air circulation, which aided oxidation of Ce<sup>3+</sup> to Ce<sup>4+</sup> and subsequently led to formation of CeO<sub>2</sub> nanoparticles [23].

In contrast, a purple coloured solution was observed for slow stirring rate (450 rpm) regardless of reaction time, suggesting that less oxidation occurred. Oxidation typically occurs once air produced from strong agitation during stirring process converts Ce<sup>3+</sup> to Ce<sup>4+</sup>. Therefore, a higher stirring rate caused rigorous agitation of the solution, thus producing more air for consumption during oxidation process, allowing more conversion of Ce<sup>4+</sup> from Ce<sup>3+</sup>. Then, available Ce<sup>4+</sup> combined with oxygen to form the yellow solid CeO<sub>2</sub> ceria. Equations (2)–(5) suggest several mechanisms for ceria nanoparticle formation, as follows:

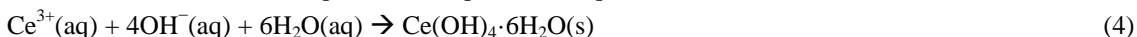
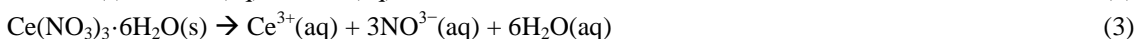


Table 1. Effect of reaction time and stirring rate towards percentage yield of ceria nanoparticle synthesis.

| Reaction Time (hours) | Stirring Rate (rpm) | Percentage Yield | Physical Observation  |
|-----------------------|---------------------|------------------|---|
| 0.5                   | 1200                | 39               | NA  |
| 1.0                   | 1200                | 43               | NA  |
| 2.0                   | 450                 | 30               | Purple solution after approximately 30 minutes of stirring                        |
| 2.0                   | 1200                | 81               | Cloudy to yellowish solution formed after approximately 30–45 minutes of stirring |
| 2.0                   | 1500                | 82               | Cloudy to yellowish solution formed after approximately 30–45 minutes of stirring |

Table 1 (cont'd). Effect of reaction time and stirring rate towards percentage yield of ceria nanoparticle synthesis.

| Reaction Time (hours) | Stirring Rate (rpm) | Percentage Yield | Physical Observation   |
|-----------------------|---------------------|------------------|--|
| 4.0                   | 1200                | 83               | Cloudy to yellowish solution formed after approximately 30–45 minutes of stirring                            |
| 8.0                   | 1200                | 84               | Cloudy to yellowish solution formed after approximately 30–45 minutes of stirring                            |
| 24.0                  | 450                 | 38               | Purple solution at the beginning and thin yellowish layer formed on top of solution after overnight stirring |
| 24.0                  | 1200                | 79               | Cloudy to yellowish solution formed after approximately 30–45 minutes of stirring                            |
| 48.0                  | 450                 | 24               | Cloudy to yellowish solution formed after approximately 30–45 minutes of stirring                            |
| 48.0                  | 1200                | 34               | Purple solution at the beginning and thin yellowish layer formed on top of solution after overnight stirring |

NA: Not Available

### X-ray diffraction

Figure 1 illustrates XRD pattern of ceria nanoparticles at different aging time, i.e.  $t = 0$  (S2),  $t = 30$  minutes (S6), and  $t = 5$  days (S3). All peaks exhibited in Figure 1 can be indexed to a pure cubic phase of  $\text{CeO}_2$  according to The Joint Committee on Powder Diffraction Standards (JCPDS file No. 34-0394). Furthermore, the XRD pattern has shown four main reflections of (111), (200), (220), and (311) of  $\text{CeO}_2$  in the cubic phase with fluorite structure. In addition, the calculated lattice constant for the synthesised sample,  $a = 0.511$  nm, matched the value from literature, namely  $a = 0.514$  nm, calculated using equation  $1/d^2 = h^2 + k^2 + l^2/a^2$  [24]. All displayed peaks have shown that the synthesised ceria nanoparticles were clean from the surfactant as no additional peaks due to other phases or impurity were detected. This resulted in a  $\text{CeO}_2$  cubic phase of high purity.

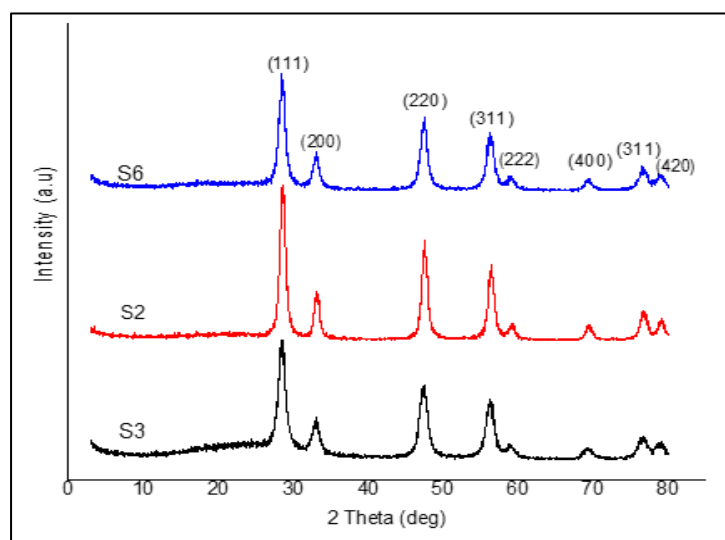


Figure 1. XRD pattern for S2, S3, and S6 samples

Findings have highlighted that at (200): (111), synthesised ceria displayed a higher intensity ratio (0.315) compared to bulk ceria (0.260). A similar trend was observed for (220): (111), whereby synthesised ceria nanoparticles' intensity ratio was 0.689, while bulk ceria's was 0.550. Thus, this trend suggests that there was better exposure for the active (100) and (110) surfaces relative to (111) surface of the synthesised ceria nanoparticles, in comparison to bulk ceria [24].

On the other hand, as tabulated in Table 2, crystallite size was between 4–12 nm, with a slight difference observed when CTAB surfactant was added. Nevertheless, aging time application is crucial for samples added with surfactant. For instance, an aging time of less than 20 days did not show any noticeable difference in crystallite size. This may be due to less or slow conversion of  $\text{Ce}^{4+}$  from  $\text{Ce}^{3+}$ , resulting in reduced  $\text{CeO}_2$  formation and directional growth.

Table 2. Crystallite size of synthesised ceria and modified ceria ( $\text{Fe-CeO}_2/\text{TiO}_2$ ) nanoparticles

| Sample                               | Surfactant | Aging Time (days) | Crystallite Size (nm) |
|--------------------------------------|------------|-------------------|-----------------------|
| $\text{CeO}_2$ (S2)                  | No         | NA                | 9.0                   |
| $\text{CeO}_2$ (S3)                  | Yes        | <1 (0.5 hours)    | 8.7                   |
| $\text{CeO}_2$ (S6)                  | Yes        | 5                 | 7.5                   |
| $\text{CeO}_2$                       | Yes        | 10                | 7.1                   |
| $\text{CeO}_2$                       | Yes        | 20                | 5.3                   |
| $\text{CeO}_2$ (S7)                  | Yes        | 30                | 4.5                   |
| $\text{Fe-CeO}_2/\text{TiO}_2$ (S10) | NA         | NA                | 11.3                  |

NA: Not Available

Importance of aging time towards nanoparticle/structure formation (Figure 2) has been reported in the literature [25]. For aging time of less than a week, no enhancement in crystallite size was noted, and this is attributable to the reaction mixture containing uniform amount of  $\text{Ce}^{3+}$  and  $\text{Ce}^{4+}$  ions. When aging time was extended to a month, significant results were observed, implying the dominance of  $\text{Ce}^{4+}$  in the reaction mixture. Therefore,  $\text{CeO}_2$  grew directionally in the presence of surfactant.

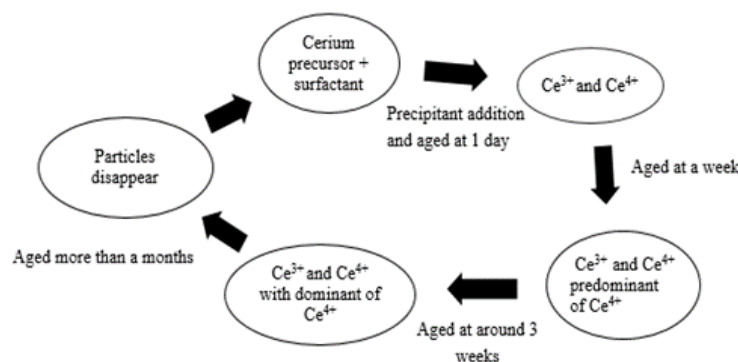


Figure 2. The proposed oxidation-reduction cycle [25]

The role played by cationic CTAB surfactant was studied by comparing samples containing and devoid of it. Sample without CTAB exhibited an unclear shape, compared to sample containing CTAB, which displayed a

sphere-like shape (Figure 3 (a) and (b)). This observation implies the influential role of CTAB in tuning the nano-shape formation. The mechanisms proposed for this observation are as follows: (i) oxidation of  $\text{Ce}^{3+}$  to  $\text{Ce}^{4+}$ ; (ii) incorporation of  $\text{Ce}^{4+}$  with cetyl-tri-methyl ammonium ion ( $\text{CTA}^+$ ); and (iii) simultaneously, exchange between  $\text{H}^+$  and alkylammonium cation (from CTAB surfactant) occurs, as per the equilibrium shown in Figure 4.

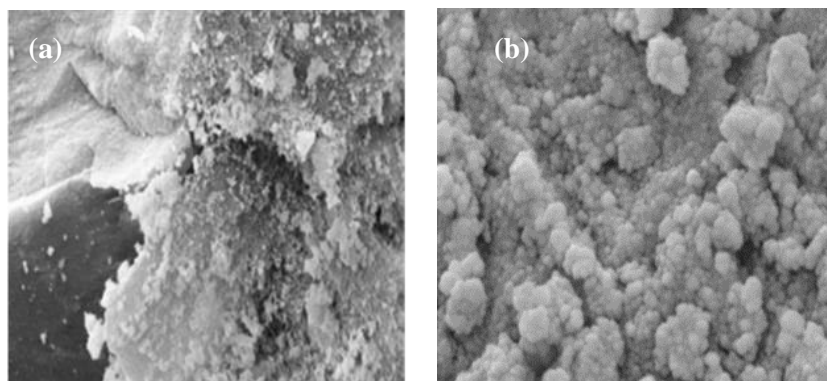


Figure 3. (a)  $\text{CeO}_2$  sample prepared without assistance of CTAB surfactant; and (b)  $\text{CeO}_2$  sample prepared with assistance of CTAB surfactant

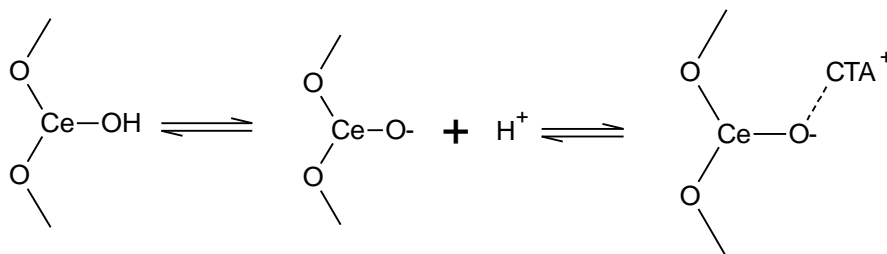


Figure 4. Reaction between alkylammonium cation (from CTAB surfactant) and cerium(IV) hydroxide

Electrostatic interaction of  $\text{Ce}-\text{O} \cdots \text{CTA}^+$  will then initiate polymerisation, which causes micellization. Excess surfactant species were expected to be adsorbed on ceria nanoparticle surface and colloidal ceria nanoparticles with surfactant would have then generated  $\text{CTA}^+$  surfactant capsule. Next, ceria/surfactant bilayers were formed due to coalescence of both organic and inorganic nanocomposites. This occurred due to inter-chain interaction between surfactant and colloidal ceria nanoparticles. Such processes enhance ceria nano-shape growth orientation [25]. Moreover,  $\text{CTA}^+$  surfactant capsule is attributable to ceria nano-shape size regulation. Finally, excess surfactant was eliminated after synthesis process via washing, to ensure the obtained sample is pure.

#### Hammet test and $\text{CO}_2$ -TPD

Before conducting  $\text{CO}_2$ -TPD, a simple acidity and basicity analysis was performed, i.e. Hammett test (Table 3). This test is a simple analysis used to roughly describe the acidity and basicity of samples. As presented in Table 3, all samples changed the colour of phenolphthalein (pH indicator; pH 8.2) from colourless to pink. In addition, two other pH indicators were also used; 4-nitroaniline (pH 18.4) and 2,4-dinitroaniline (pH 15.0); however, no colour changes were observed. Therefore, these preliminary results suggest that all the samples were not acidic in nature while the basicity was in the range of  $8.2 < \text{pH} < 15.0$ . Since Hammett test provided the basicity range for all the samples, TPD analysis was continued with  $\text{CO}_2$ -TPD.

Table 3. Hammet test analysis for S2, S3, and S6

| Catalyst | Phenolphthalein    | 2,4-dinitroaniline | 4-nitroaniline    |
|----------|--------------------|--------------------|-------------------|
| S2       | Colourless to pink | No colour changes  | No colour changes |
| S3       | Colourless to pink | No colour changes  | No colour changes |
| S6       | Colourless to pink | No colour changes  | No colour changes |

CO<sub>2</sub>-TPD was conducted on S2, S3, and S6 samples and the total CO<sub>2</sub> gas desorbed were 18.56, 2211.19, and 2076.00  $\mu\text{mol/g}$ , respectively. Figure 5 and Table 4 both depict the peaks exhibited by all three samples. The CO<sub>2</sub>-TPD technique can be classified according to type, as follows:

peaks at <200°C : weak basic sites;  
 peaks at 200°C–400°C : medium basic sites; and  
 peaks >400°C : strong basic sites.

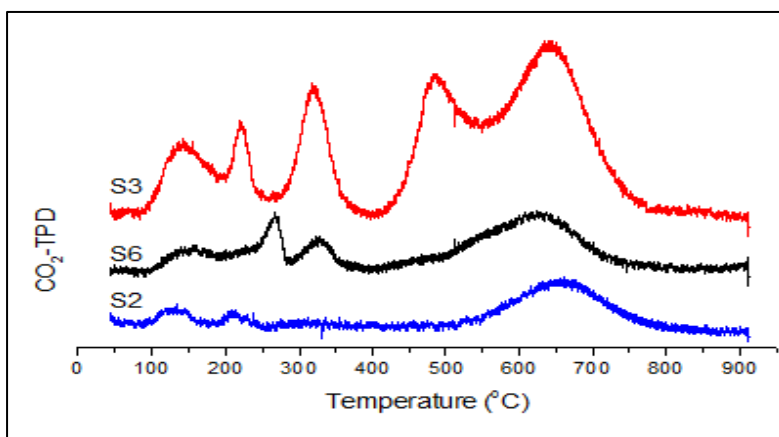


Figure 5. CO<sub>2</sub>-TPD for S2, S3, and S6

Table 4. Total CO<sub>2</sub> desorption for S2, S3, and S6

| Sample | Peak (°C) | Total CO <sub>2</sub> Desorption (%) |
|--------|-----------|--------------------------------------|
| S2     | 662       | 100                                  |
| S3     | 145       | 6                                    |
|        | 223       | 6                                    |
|        | 321       | 13                                   |
|        | 491       | 18                                   |
|        | 645       | 57                                   |
| S6     | 162       | 2                                    |
|        | 267       | 58                                   |
|        | 624       | 40                                   |

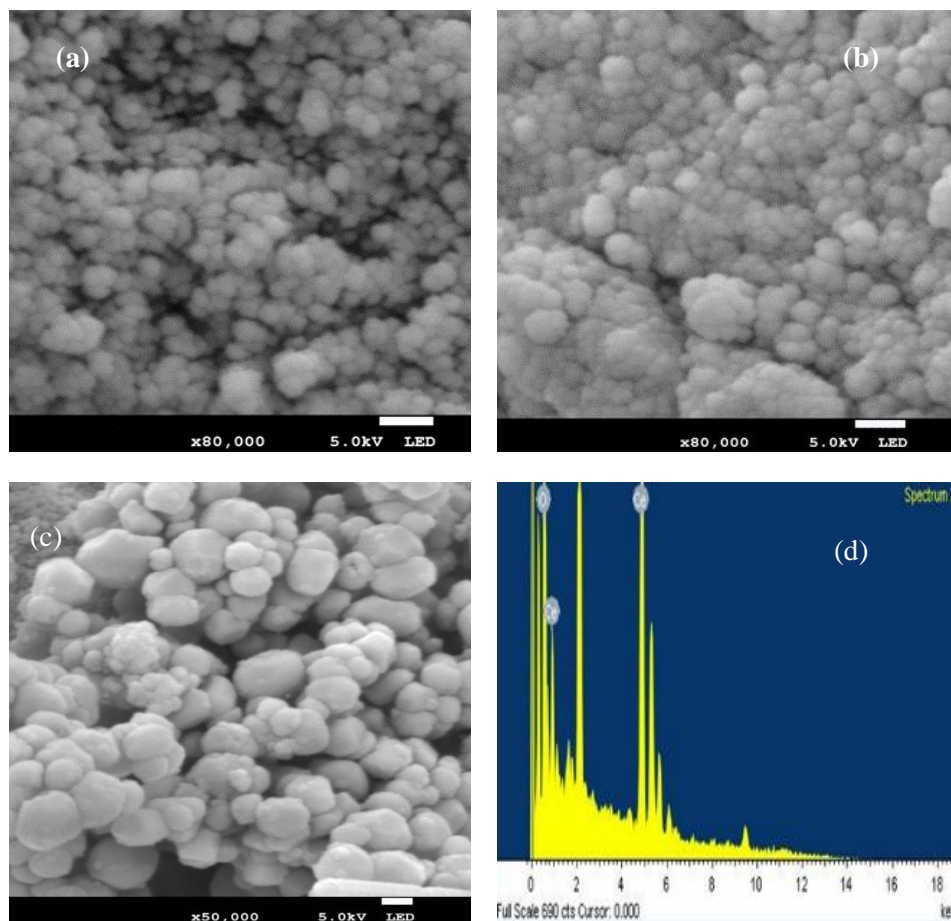


Sample S3 exhibited peaks at 145°C, 223°C, 321°C, 491°C, and 645°C, indicating the presence of strong basic sites. Nonetheless, additional mild basic site peaks observed at 223°C and 491°C may also imply formation of inorganic and/or organic species, causing reaction between surfactant and deprotonated OH<sup>-</sup> group [26]. As such, this preliminary result suggests that longer aging time may have influenced the sample's basic sites, as it led to stronger interface interaction between cationic surfactant and ceria surface nanoparticles. Hence, the cationic part of surfactant may have acted as a Lewis acid and altered the basic sites.

#### Field emission scanning electron microscopy

High resolution FESEM analysis was carried out to study the morphology and elemental composition of synthesised ceria and modified ceria, Fe-CeO<sub>2</sub>/TiO<sub>2</sub>, nanoparticles. Figure 6 (a-c) shows that both samples did not agglomerate and form a sphere-like structure. On the other hand, Figure 6(d) reveals that synthesised ceria nanoparticles contained only Ce and O elements, which concur with XRD results. Meanwhile, Figure 6(e) exhibits the EDX spectrum of Fe-CeO<sub>2</sub>/TiO<sub>2</sub> that proves the presence of Fe and Ti elements in the sample.

Nevertheless, due to technique-related limitations, presence of other ions originating from the surfactant cannot be ruled out. The ions were expected to be adsorbed at the surface, but its adsorption effect on ceria surface was weak and negligible [27]. In addition, Figure 6(c) illustrates the clear sphere-like shape observed. This indicates the interaction between Fe ion with the basic surface of CeO<sub>2</sub>, contributing towards CeO<sub>2</sub> nanoparticles tuning shape process. Thus, CeO<sub>2</sub> surface's mild to high range of basicity was expected to enhance the electrostatic interaction occurring between Fe ion and CeO<sub>2</sub> surface.



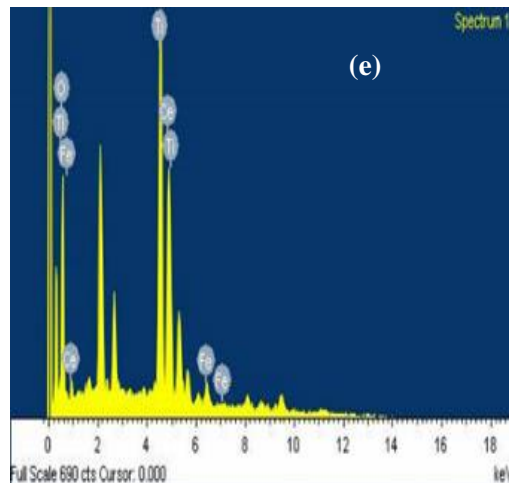


Figure 6. FESEM images of ceria and modified ceria nanoparticles: (a) S3 sample; (b) S7 sample; (c) S10 sample; (d) EDX spectrum of synthesised  $\text{CeO}_2$  sample from different areas; and (e) EDX spectrum of  $\text{Fe-CeO}_2/\text{TiO}_2$  particle sample

### Conclusion

$\text{CeO}_2$  nanoparticles and modified  $\text{CeO}_2$ ,  $\text{Fe-CeO}_2/\text{TiO}_2$ , were successfully synthesised using precipitation and impregnation methods, respectively. Synthesised  $\text{CeO}_2$  nanoparticles produced crystallite sized between 4–18 nm and showed no agglomeration in FESEM images. Meanwhile, modified  $\text{CeO}_2$  nanoparticles with iron metal loading and titania ( $\text{TiO}_2$ ) as support formed a sphere-like shape, with the presence of Fe and Ti confirmed by EDX spectrum. Additionally, synthesis of ceria hybrid and  $\text{CeO}_2$  using other surfactants and substrates like polyvinyl alcohol (PVA) could be an interesting prospective study. Other than that, previous research reported on synthesis of a particular material hybrid nanoparticle, which provided significant enhancement for properties like hardness and heat resistance [28–30]. Therefore, in future, comprehensive study on  $\text{CeO}_2$  hybrid nanoparticle synthesis with PVA surfactant will be considered.

### Acknowledgement

This work is supported by Universiti Malaysia Pahang, the Ministry of Education, Malaysia for Exploratory Research Grant Scheme (ERGS) (RDU 120605), and Malaysia Toray Science Foundation (RDU 141501). The first author would like to thank the Ministry of Education, Malaysia for their support via MyPhD funding.

### References

1. Sayyed, S. A., Beedri, N. I., Kadam, V. S. and Pathan, H. M. (2016). Rose bengal-sensitized nanocrystalline ceria photoanode for dye-sensitized solar cell application. *Bulletin of Materials Science*, 39(6): 1381-1387.
2. Namjesnik, D., Mutka, S., Iveković, D., Gajović, A., Willinger, M. and Preočanin, T. (2016). Application of the surface potential data to elucidate interfacial equilibrium at ceria/aqueous electrolyte interface. *Adsorption*, 22(4-6): 825-837.
3. Eltayeb, A., Vijayaraghavan, R. K., McCoy, A., Venkatanarayanan, A., Yaremchenko, A. A., Surendran, R. and Daniels, S. (2015). Control and enhancement of the oxygen storage capacity of ceria films by variation of the deposition gas atmosphere during pulsed DC magnetron sputtering. *Journal of Power Sources*, 279: 94-99.
4. Li, H., Hu, T., Liu, J., Song, S., Du, N., Zhang, R. and Hou, W. (2016). Thickness-dependent photocatalytic activity of bismuth oxybromide nanosheets with highly exposed (010) facets. *Applied Catalysis B: Environmental*, 182: 431-438.
5. Gao, G.-M., Zou, H.-F., Liu, D.-R., Miao, L.-N., Ji, G.-J. and Gan, S.-C. (2009). Influence of surfactant surface coverage and aging time on physical properties of silica nanoparticles. *Colloids and Surfaces A: Physicochemical and Engineering Aspects*, 350(1): 33-37.

6. Das, D., Llorca, J., Dominguez, M., Colussi, S., Trovarelli, A. and Gayen, A. (2015). Methanol steam reforming behavior of copper impregnated over CeO<sub>2</sub>-ZrO<sub>2</sub> derived from a surfactant assisted coprecipitation route. *International Journal of Hydrogen Energy*, 40(33): 10463-10479.
7. Vantomme, A., Yuan, Z.-Y., Du, G. and Su, B.-L. (2005). Surfactant-assisted large-scale preparation of crystalline CeO<sub>2</sub> nanorods. *Langmuir*, 21(3): 1132-1135.
8. Pan, C., Zhang, D. and Shi, L. (2008). CTAB assisted hydrothermal synthesis, controlled conversion and CO oxidation properties of CeO<sub>2</sub> nanoplates, nanotubes, and nanorods. *Journal of Solid State Chemistry*, 181(6): 1298-1306.
9. Ebadi, M., Amiri, O. and Sabet, M. (2018). Synthesis of CeO<sub>2</sub>/Au/Ho nanostructures as novel and highly efficient visible light driven photocatalyst. *Separation and Purification Technology*, 190: 117-122.
10. Liu, Q., Ding, Y., Yang, Y., Zhang, L., Sun, L., Chen, P. and Gao, C. (2016). Enhanced peroxidase-like activity of porphyrin functionalized ceria nanorods for sensitive and selective colorimetric detection of glucose. *Materials Science and Engineering: C*, 59: 445-453.
11. Younis, A., Chu, D., Kaneti, Y. V. and Li, S. (2016). Tuning the surface oxygen concentration of {111} surrounded ceria nanocrystals for enhanced photocatalytic activities. *Nanoscale*, 8(1): 378-387.
12. Zhang, D., Fu, H., Shi, L., Pan, C., Li, Q., Chu, Y. and Yu, W. (2007). Synthesis of CeO<sub>2</sub> nanorods via ultrasonication assisted by polyethylene glycol. *Inorganic Chemistry*, 46(7): 2446-2451.
13. Terribile, D., Trovarelli, A., Llorca, J., de Leitenburg, C. and Dolcetti, G. (1998). The synthesis and characterization of mesoporous high-surface area ceria prepared using a hybrid organic/inorganic route. *Journal of Catalysis*, 178(1): 299-308.
14. Ramasamy, V. and Vijayalakshmi, G. (2016). Synthesis and characterization of ceria quantum dots using effective surfactants. *Materials Science in Semiconductor Processing*, 42: 334-343.
15. Yang, R. and Guo, L. (2005). Synthesis of cubic fluorite CeO<sub>2</sub> nanowires. *Journal of Materials Science*, 40(5): 1305-1307.
16. Choi, M., Na, K., Kim, J., Sakamoto, Y., Terasaki, O. and Ryoo, R. (2009). Stable single-unit-cell nanosheets of zeolite MFI as active and long-lived catalysts. *Nature*, 461 (7261): 246-249.
17. Lin, K.-S. and Chowdhury, S. (2010). Synthesis, characterization, and application of 1-D cerium oxide nanomaterials: A review. *International Journal of Molecular Sciences*, 11(9): 3226-3251.
18. Torrente-Murciano, L., Chapman, R. S., Narvaez-Dinamarca, A., Mattia, D. and Jones, M. D. (2016). Effect of nanostructured ceria as support for the iron catalysed hydrogenation of CO<sub>2</sub> into hydrocarbons. *Physical Chemistry Chemical Physics*, 18(23): 15496-15500.
19. Laosiripojana, N., Assabumrungrat, S. and Charojrochkul, S. (2007). Steam reforming of ethanol with Co-Fed oxygen and hydrogen over Ni on high surface area ceria support. *Applied Catalysis A: General*, 327(2): 180-188.
20. Yao, S., Xu, W., Johnston-Peck, A., Zhao, F., Liu, Z., Luo, S. and Rodriguez, J. (2014). Morphological effects of the nanostructured ceria support on the activity and stability of CuO/CeO<sub>2</sub> catalysts for the water-gas shift reaction. *Physical Chemistry Chemical Physics*, 16(32): 17183-17195.
21. Yoshida, T., Murachi, M., Tsuji, S. and Taguchi, N. (1999). High heat-resistant catalyst with a porous ceria support. U.S. Patent and Trademark Office, Washington, DC.
22. Li, H., Wang, G., Zhang, F., Cai, Y., Wang, Y. and Djerdj, I. (2012). Surfactant-assisted synthesis of CeO<sub>2</sub> nanoparticles and their application in wastewater treatment. *RSC Advances*, 2(32): 12413-12423.
23. Wang, J., Liu, Q. and Liu, Q. (2008). Ceria-and Cu-doped ceria nanocrystals synthesized by the hydrothermal methods. *Journal of the American Ceramic Society*, 91(8): 2706-2708.
24. Deori, K., Gupta, D., Saha, B., Awasthi, S. K. and Deka, S. (2013). Introducing nanocrystalline CeO<sub>2</sub> as heterogeneous environmental friendly catalyst for the aerobic oxidation of para-xylene to terephthalic acid in water. *Journal of Materials Chemistry A*, 1(24): 7091-7099.
25. Karakoti, A. S., Munusamy, P., Hostetler, K., Kodali, V., Kuchibhatla, S., Orr, G. and Baer, D. R. (2012). Preparation and characterization challenges to understanding environmental and biological impacts of ceria nanoparticles. *Surface and Interface Analysis*, 44(8): 882-889.
26. Indran, V. P., Zuhaimi, N. A. S., Deraman, M. A., Maniam, G. P., Yusoff, M. M., Hin, T.-Y. Y. and Rahim, M. H. A. (2014). An accelerated route of glycerol carbonate formation from glycerol using waste boiler ash as catalyst. *RSC Advances*, 4(48): 25257-25267.

27. Huang, X.-S., Sun, H., Wang, L.-C., Liu, Y.-M., Fan, K.-N. and Cao, Y. (2009). Morphology effects of nanoscale ceria on the activity of Au/CeO<sub>2</sub> catalysts for low-temperature CO oxidation. *Applied Catalysis B: Environmental*, 90(1): 224-232.
28. Aziz, R. C. A., Ab Rahman, I. and Mohamad, D. (2012). Synthesis of silica hybrid nanoparticles and the effect of their addition on the hardness of the dental nanocomposites. *International Journal on Advanced Science, Engineering and Information Technology*, 2(3): 211-214.
29. Yunus, M., Suharyadi, E. and Triyana, K. (2016). Effect of stirring rate on the synthesis silver nanowires using polyvinyl alcohol as a capping agent by polyol process. *International Journal on Advanced Science, Engineering and Information Technology*, 6(3): 365-369.
30. Zain, N. M., Rashdi, N. M., Ubaidillah, N. K. A. N. and Azmi, M. S. (2016). The effect of carbon nanotube loading on wettability of solder paste SAC 237 and different substrates. *International Journal on Advanced Science, Engineering and Information Technology*, 6(4): 540-543.